Synthesis of a Conducting SiO_2−Carbon Composite from Commercial Silicone Grease and Its Conversion to Paramagnetic SiO_2 Particles

V. G. Pol, S. V. Pol, P. P. George, B. Markovsky, and A. Gedanken*

Department of Chemistry and Kanbar Laboratory for Nanomaterials at the Bar-Ilan University Center for Advanced Materials and Nanotechnology, Bar-Ilan University, Ramat-Gan, 52900, Israel

Received: February 13, 2006; In Final Form: May 12, 2006

The thermal decomposition of commercial silicone grease was carried out in a closed reactor (Swagelok) that was heated at 800 °C for 3 h, yielding a SiO_2−carbon composite with a BET surface area of 369 m^2/g. The bulk conductivity (5.72×10^{-6} $S \cdot cm^{-2}$) of the SiO_2−carbon composite was determined by impedance measurements. The as-prepared SiO_2−carbon composite was further annealed at 500 °C in air for 2 h, which led to the formation of white paramagnetic silica particles (confirmed by ESR), possessing a surface area of 111 m^2/g. The present synthetic technique requires unsophisticated equipment and a low-cost commercial precursor, and the reaction is carried out without a solvent, surfactant, or catalyst. The mechanism for the formation of a porous SiO_2−carbon composite from the silicone grease is also presented.

Introduction

Carbon and silica play an important role in chemistry, physics, and materials science due to their relevance in practical applications and academic research.[1] More than a thousand original papers and reviews on this topic have been reported.[2−5] Carbon exhibits a very rich structural and surface chemistry.[2,3,6] Various different architectures are possible because carbon can bind in linear (sp), trigonal (sp^2), and tetrahedral (sp^3) coordinations. Many crystalline and amorphous forms have been synthesized, such as glassy carbon, fibers, films, and nanotubes.[2,3,6−8]

Silica−carbon composite materials are very interesting because of their high electrical conductivity, intercalating capability, high thermal stability, and high resistance to organic solvents.[6−8] Hybrid materials consisting of a graphite-like carbon phase and an inorganic oxidic component can be synthesized by different strategies. A convenient route for synthesizing the carbon component is the thermal transformation of a suitable organic precursor polymer into the carbon phase.[9−11] Interpenetrating carbon/silica hybrid materials have been obtained by a sol−gel process of tetraalkoxysilanes using water-soluble monomers or oligomers, which are suitable as carbon precursor materials.[12,13] These materials are important for various applications, because each component serves as the template for the other. Mastai et al. reported a new concept, i.e., that silica−carbon nanocomposites can act as solar absorbers.[14] Recently, Pang et al. synthesized hierarchical mesoporous carbon/silica nanocomposites from phenyl bridged organosilane.[15] The preparation and characterization of silica−carbon hybrids are carried out by initially adsorbing silicon tetrachloride onto the surface of porous carbon particles.[16] The experimental evaluation of the optical properties of porous silica/carbon composite particles was demonstrated by Chang[17] et al. Previously, the paramagnetic silica nanoparticles were prepared by doping Gd^{3+} ions bound in a *n*-(trimethoxysilylpropyl)ethyldiamine triacetic acid trisodium salt [TSPETE] and used for mutimodal bioimaging.[18]

In this paper, we report on a one-stage, catalyst-free, efficient and simple synthetic technique, using a commercially available nonconventional single precursor, silicone grease, for the production of high surface area carbon silica hybrid materials. The as-prepared SiO_2−carbon composite is a conducting material, as determined by impedance measurements. The thermal decomposition of silicone grease at 800 °C in a closed Swagelok cell under inert atmosphere yielded a SiO_2−carbon composite. Following this step, the annealing of the product at 500 °C in air led to the formation of white paramagnetic SiO_2 particles. Recently, a variety of interesting nanostructures have been reported for various organic/inorganic precursors[19] with their RAPET (reactions under autogenic pressure at elevated temperature) reactions. The results of the current research suggest that a small amount (∼2 wt %) of silicone grease should be added during sintering of magnetic materials. This addition might prevent, for example, the agglomeration of magnetic nanoparticles during their sintering.

Experimental Section

Synthesis of SiO_2−Carbon Composite and SiO_2 Particles. The fabrication of a SiO_2−carbon composite is carried out by introducing the silicone grease (silicaid 1010, Aidchim Ltd., Israel) into a 2 mL closed vessel cell. Silicaid (1010) is a grease-like silicone compound with high thermal conductivity, good water repellency, excellent insulation properties, low surface tension, and good stability at high temperatures. The reaction cell is assembled from stainless steel Swagelok parts. A 1/2 in. union part is capped from both sides by standard plugs. For these syntheses, 1 g of silicaid 1010 is introduced into the cell at room temperature under nitrogen (nitrogen-filled glovebox). The filled cell is closed tightly by the other plug and then placed inside an iron pipe (inner diameter 3 in.) in the middle of the furnace. The temperature is raised at a heating rate of 10 °C/min. The closed vessel cell is heated at 800 °C for 3 h. The reaction takes place under the autogenic pressure of the precursor. The Swagelok is gradually cooled (∼5 h) to room temperature, then it is opened, and a pale-yellow powder is obtained. The total yield of product material is about 70% of the total weight of silicone grease introduced in the cell. (The yield is defined as the final weight of the product relative to

* Corresponding author. E-mail: gedanken@mail.biu.ac.il.

10.1021/jp060919q CCC: $33.50
Published on Web 06/16/2006

the weight of silicaid 1010, the starting material.) The as-prepared SiO_2−carbon composite is further annealed at 500 °C in air. The annealing leads to the formation of white silica particles. The possibility of dissolving silica from a SiO_2−carbon composite in 20% HF acid, keeping carbon as a sole product, is also demonstrated.

Characterization. The X-ray diffraction pattern of the products were measured with a Bruker AXS D* Advance powder X-ray diffractometer (using Cu Kα = 1.5418 Å radiation). The elemental analysis of the SiO_2−carbon composite and SiO_2 sphere samples was carried out on an Eager 200 C, H, N, S analyzer. The elemental composition of the materials and the scanning electron microscopic (SEM) image were analyzed by an energy-dispersive X-ray (EDX) analysis technique attached to a JEOL-JSM 840 scanning electron microscope. The porous particle morphology and the disordered structures were studied by transmission electron microscopy (TEM) on a JEOL-JEM 100 SX microscope, working at an 80 kV accelerating voltage, and with a JEOL-2010 high-resolution (HR) TEM instrument, using an accelerating voltage of 200 kV. Samples for TEM and HR-TEM were prepared by ultrasonically dispersing the SiO_2−carbon composite and SiO_2 particles into absolute ethanol, placing a drop of this suspension onto a copper grid coated with an amorphous carbon film, and then drying in air. An Olympus BX41 (Jobin Yvon Horiba) Raman spectrometer was employed, using the 514.5 nm line of an Ar ion laser as the excitation source to analyze the nature of the carbon present in the SiO_2−carbon composite. A Micromeritics (Gemini 2375) surface area analyzer was used to measure the surface area of the SiO_2−carbon composite and SiO_2 sphere samples. Electron paramagnetic resonance (EPR) spectra were recorded on a Bruker EPR spectrometer (ER083 CS) operating at an X-band (υ = 9.77 GHz) with a 100 kHz magnetic field modulation. The electrochemical measurements were carried out using a battery test unit Model 1470 coupled with a FRA Model 1255 from Solartron, Inc. (driven by Corrware and ZPlot software from Scribner Assoc.). The alternating voltage amplitude in impedance measurements was 3 mV, and the alternating current frequency range used was 50 kHz to 100 Hz. The silica−carbon sample pellet (geometric area around 3.1 cm^2) was prepared at a pressure of 3000 psi.

Results and Discussion

Systematic compositional, structural, morphological, magnetic characterization, and surface area measurements were carried out to understand the reaction products. The content of carbon and hydrogen in the product/carbonaceous material was determined by an elemental analysis measurement. We measured the element (weight) percent of carbon and hydrogen in the SiO_2−carbon composite and in silica particles. The measured element (weight) percentage of carbon in the as-prepared product was 9.6% (in 0.700 g of product). The weight loss of the SiO_2−carbon composite measured by thermogravimetric analysis (TGA) in an air atmosphere was ~9.2% in the temperature range of 300−500 °C. This means that the SiO_2:C ratio is approximately 9:1. From this observation, the SiO_2−carbon composite was annealed at 500 °C in air for 2 h, which led to the formation of pure silica particles. The measured amount of carbon was <1%. The amount of hydrogen in both products (as-prepared and annealed in air at 500 °C) was negligible.

The measurement of the dispersive X-ray analysis (EDX) substantiated the chemical analysis results. For the SiO_2−carbon composite sample, the peaks indicated the presence of C, Si, and O [Figure 1a], and no evidence was found for any other impurity. The SiO_2−carbon composite, which was burned at 500 °C/air/2 h, revealed that <1 wt % carbon is still present in the silica [Figure 1b]. To get rid of the silica, the SiO_2−carbon composite was dissolved in a 20% HF solution to form pure carbon. Only the presence of carbon was evidenced by the EDX spectrum shown in Figure 1c.

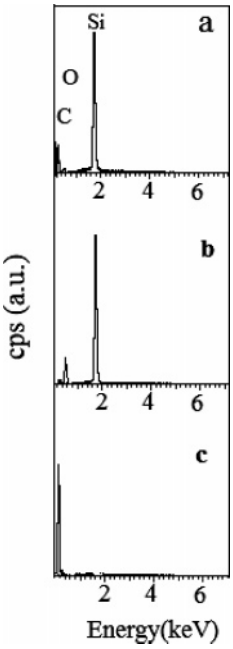

Figure 1. EDX spectra of (a) a SiO_2−carbon composite, (b) silica particles, and (c) leftover carbon particles after dissolution of silica from a SiO_2−carbon composite in 20% HF acid.

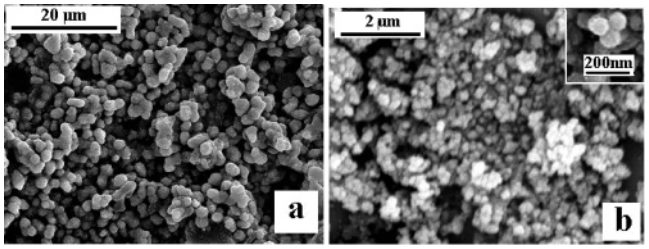

Figure 2. SEM images of (a) an as-prepared SiO_2−carbon composite and (b) silica particles.

The powder X-ray diffraction (XRD) measurement depicts the broad background at 2θ angles between 20 and 30°, showing the presence of amorphous silica [data not shown]. The low-angle XRD does not show any peak, thus preventing the possibility of structural ordering.

The SEM image of the product obtained after the thermal decomposition of silicone grease at 800 °C is presented in Figure 2a. It indicates that the particles are not completely spherical, but possess an average diameter of 2−3 μm. The surfaces of SiO_2−carbon composite particles are also not smooth. The as-prepared SiO_2−carbon composite was further annealed at 500 °C in air for 2 h. A drastic reduction in the particle diameter was observed, which might be due to the burning of the carbon. These silica particles have a diameter of 80−150 nm [Figure 2b]. The spherical particles of silica with an 80 nm diameter are also presented under large magnification [insert of Figure 2b].

To further learn about the morphology of the as-prepared product, TEM measurements were conducted. They revealed amorphous aggregates of around 200 nm [Figure 3a], demonstrating the typical morphology of the silica−carbon composite. A porous nature was observed for the silica−carbon composite

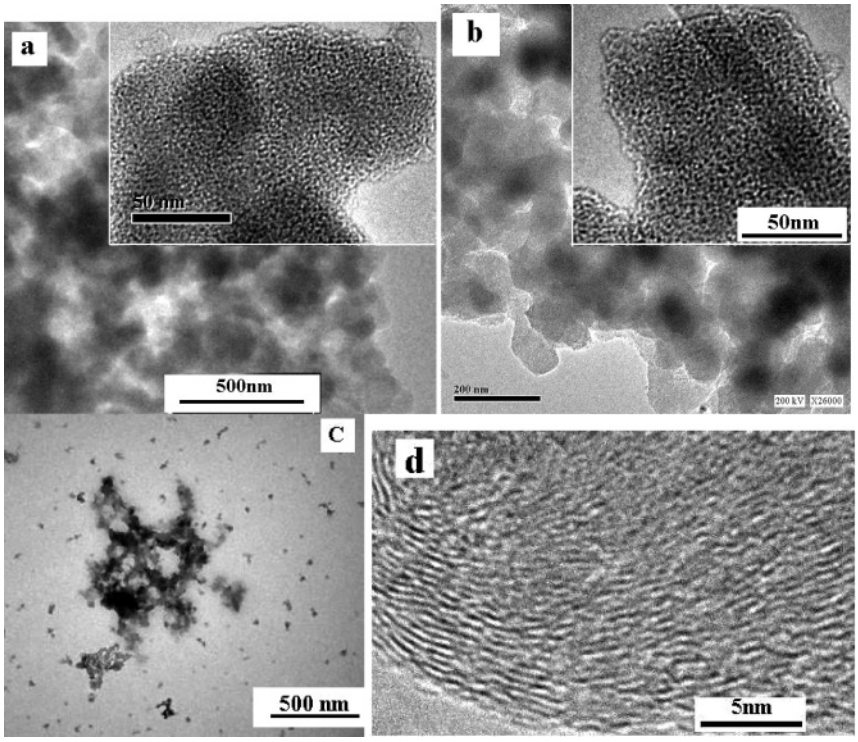

Figure 3. TEM pictures of (a) SiO_2−carbon composite (insert, HR-TEM), (b) silica particles received after burning the carbon (insert, HR-TEM), (c) leftover carbon particles after dissolution of silica from the SiO_2−carbon composite in 20% HF acid, and (d) HR-TEM of the edge of the carbon particles observed in (c).

in the high-resolution TEM image presented as an insert image. The observed high surface area (369 m^2/g) is explained by the porous structure of the composite. The successful removal/burning of carbon was carried out by annealing the SiO_2−carbon composite at 500 °C/air/2 h. The remaining silica particles are spheroidal in shape and in the range of 80−150 nm in size. The removal of carbon from the SiO_2−carbon composite maintains the porous nature of silica particles, evidenced by the high-resolution image shown in the insert. It is interesting to note that the SiO_2−carbon composite is dissolved in 20% HF acid, the silica particles dissolve, and around 9% by weight carbon is left over. Such carbon particles have a particle diameter of 10−12 nm [Figure 3c] and are found in the form of aggregates or as separate carbon nanoparticles, as evidenced by TEM measurements. The HR-TEM image of the leftover carbon particles after the dissolution of silica from the SiO_2−carbon composite in 20% HF is presented in Figure 3d. The ordered and disordered carbon layers are observed at the edge of the carbon particle. The interlayer spacing between the ordered carbon layers (0.334) is very close to the distance between the graphitic layers.

The N_2 adsorption−desorption isotherm of the SiO_2−carbon composite that was prepared at 800 °C after thermal decomposition of silicaid 1010 is presented in Figure 4a. The absorption and desorption isotherms exhibit an abrupt change when the relative pressure is greater than 0.9, indicating the porous nature of the sample.[20] The calculated BET surface area is 369 m^2/g, and a large pore volume of 0.15 cm^3/g is recorded. The sintered SiO_2−carbon composite at 500 °C/air/2 h led to the formation of white silica particles [Figure 4b] with a surface area of only 111 m^2/g. This sudden drop/reduction in the surface area, as compared with the SiO_2−carbon composite, is due to the burning of the carbon.

Some of the direct evidence for the formation of silica from silicone grease is obtained by Fourier transform infrared (FT-IR) measurements. The FT-IR spectrum of the SiO_2−carbon

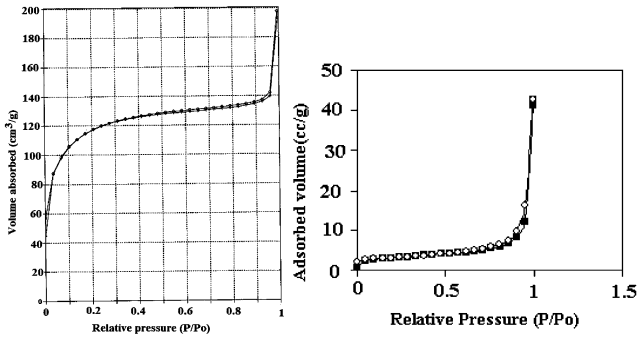

(a) (b)

Figure 4. N_2 adsorption−desorption isotherms of (a) SiO_2−carbon composite and (b) silica particles.

composite is shown in Figure 5a. The silica particles obtained after annealing the SiO_2−carbon composite at 500 °C in air [Figure 5b] and bare silica spheres [Figure 5c] prepared by Stöber's method[21] showed almost identical absorption bands. In general, the silica spheres showed four different absorption bands in the spectral region of 400−4000 cm^{-1}. The assignment of absorption bands of silica can be made by understanding the complex surface structure. Silica is composed of $[SiO]_4$ tetrahedra linked together, so that every oxygen atom is common to two tetrahedra. The surface of the as-made Stöber's silica usually contains four types of oxygen species:[22,23] (a) the oxygen associated with single free silanols, (b) oxygen in the network of hydrogen-bonded silanols, (c) silanol oxygen bonded to the physisorbed water, and (d) the bridging oxygen in the siloxane links (Si−O−Si). The broad band between 3700 and 2700 cm^{-1} corresponds to the OH stretching of surface silanols[31] (a, b, and c types of bonding). The absorption band at ∼460 cm^{-1}corresponds to the rocking mode, while the band at ∼810 cm^{-1} is due to symmetric stretching of the Si−O−Si group.[31] The broad doublet band in the region of 1300−900 cm^{-1} corresponds to

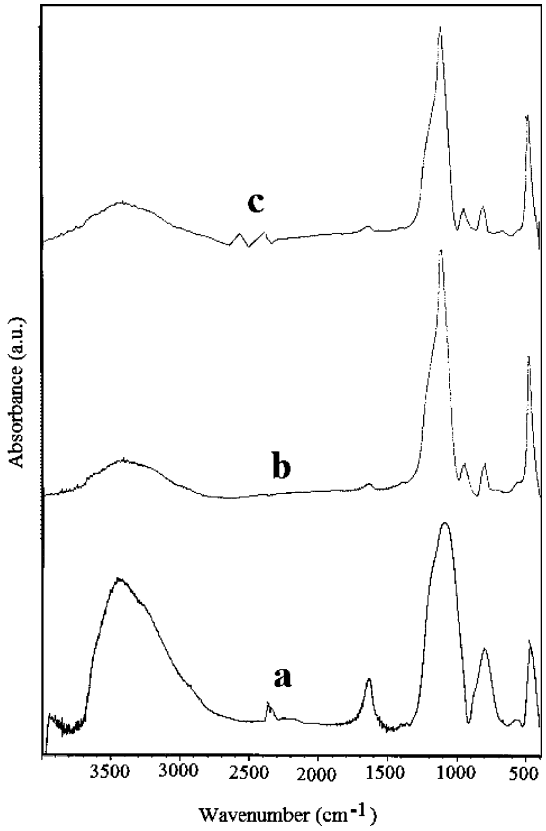

Figure 5. FT-IR spectra of (a) SiO_2−carbon composite, (b) formed silica particles after annealing SiO_2−carbon composite at 500 °C in air, and (c) bare silica spheres prepared by Stöber's method.

the asymmetric stretching vibrational mode of the Si−O−Si bridge of the siloxane link. The band appearing at 1060 cm^{-1} corresponds to the characteristic oxygen asymmetric stretching (AS) mode.

On the other hand, the silica−carbon composite [Figure 5a] shows some unique absorption bands, which are not observed in the spectra of the other silicas measured for comparison. The main difference is the formation of a broad single band instead of the doublet band in the wavenumber region of 1300−900 cm^{-1}, corresponding to the asymmetric stretching vibrational mode of the Si−O−Si bridge of the siloxane link. This is explained as being due to the change of the Si−O−Si bridge into Si−O−C, which might have led to the broad single band. An increase in the intensity of the absorption band at 1640 cm^{-1} is attributed to the strong asymmetric oxygen stretching caused by the surrounding carbon on the surface of the silica particles.

To understand the nature of the carbon present in the silica−carbon composite, Raman spectroscopic measurements were performed. The micro-Raman spectrum of this composite is presented in Figure 6a. The two characteristic bands[24] of carbon were detected at 1339 cm^{-1} (D-band), and at 1595 cm^{-1} (G-band). The intensity of the G-band, associated with graphitic edge planes and carbon dangling bonds, was slightly more intense than the D-band, associated with a disordered band, for the silica−carbon composite.

The Raman measurement of bare carbon nanoparticles, obtained by dissolving the silica, was also carried out and is presented in Figure 6b. The two characteristic bands[24] of carbon were detected at 1337 cm^{-1} (D-band) and 1592 cm^{-1} (G-band). We observed an increase in the intensity of the G-band associated with the graphitic nature of the carbon nanoparticles. This is in good agreement with the observed structural evidence obtained by HR-TEM of carbon particles [Figure 3d].

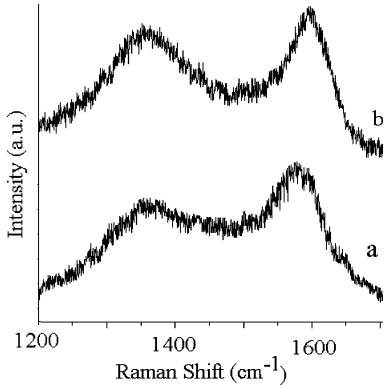

Figure 6. Raman spectra of (a) silica−carbon composite and (b) leftover carbon particles after dissolution of silica from SiO_2−carbon composite in 20% HF acid.

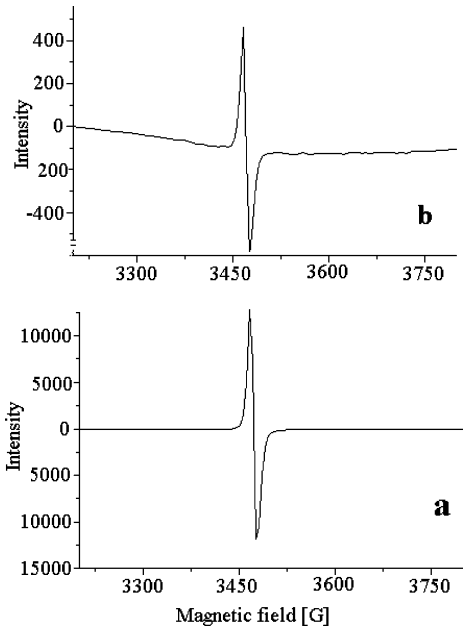

Figure 7. EPR spectra of (a) silica−carbon composite and (b) silica particles taken at room temperature.

The EPR spectra of the silica−carbon composite and silica particles were taken at room temperature and are shown in Figure 7. The *g*-factor is a dimensionless constant and is equal to 2.002 39 for the unbound electron.[25a] The silica−carbon composite showed a peak-to-peak separation (ΔH_{pp}) of ∼45 G and a *g*-value of 2.009. The silica particles showed a peak-to-peak separation (ΔH_{pp}) of 40 G and a *g*-value of 2.0071. These narrow paramagnetic[25b] resonance signals (width ∼40 G) match the non-graphitized carbon black reported by Mrozowski. Interestingly, silica particles also showed the unusual ESR signal. This signal might have originated from the trace carbon (<1%) left in the silica particles after burning the silica−carbon composite for 500 °C/2 h. Even after the long-time sintering at a higher temperature [24 h/600 °C] of the silica−carbon composite, 0.6 wt % carbon remains in the silica particles [confirmed by C, H, N, S analysis], which might have been trapped inside. The intensity of the EPR signal in the silica−carbon composite is 3 times stronger than the signal of the silica particles. The detection of paramagnetic silica nanoparticles was reported earlier.[18] They were synthesized by trapping magnetic Gd^{3+} ions in TSPETE [*n*-(trimethoxysilylpropyl)ethyldiamine triacetic acid trisodium salt] complex, and found application in multimodal bioimaging.[18]

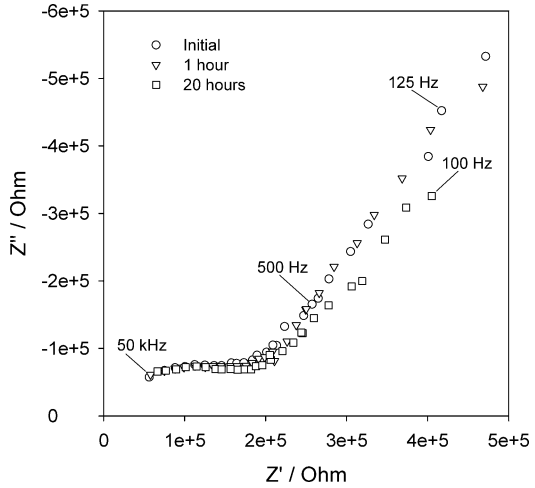

Figure 8. Family of impedance spectra (Nyquist plots) measured at room temperature from a SiO_2−carbon composite electrode at the initial time and after 1 and 20 h (for a silica−carbon composite).

It is known that silica acts as an insulator and that the conducting properties of silica can be improved through doping it with electrolytes.[26] The bulk conductivity of the silica−carbon composite was determined by impedance measurements in the frequency range of 50 kHz to 100 Hz [Figure 8]. The results obtained for the SiO_2−carbon composite demonstrated that the impedance is almost invariant with the time of the measurements in the high-frequency domain, and changes slightly in the low-frequency domain. From these measurements, at $f = 50$ kHz, the calculated value of conductivity is around 5.72×10^{-6} $S \cdot cm^{-2}$. This observed conductivity is probably due to homogeneously dispersed semi-graphitic carbon within the silica pores. Recently, there was a report on the rapid synthesis of monodispersed, conducting solid microsilica spheres by hydrolyzing tetramethyl orthosilicate (TMOS) and tetraethyl orthosilicate (TEOS) in an ionic liquid, 1-butyl-3-methylimidazolium hexafluorophosphate, at room temperature.[27] They reported that the conductivity at 5 kHz at room temperature is 7.87×10^{-6} $S \cdot cm^{-2}$.

The possible mechanism for the formation of a silica−carbon composite can be explained as follows. Silicaid grease (a silicone compound) is a material containing dimethyl polysiloxane fluids and inert silica as a filler. The thermal decomposition of silicaid grease at 700 °C yielded a mixture of SiO_2, SiO, and carbon. When the Swagelok containing this mixture was opened to air, the SiO converted to SiO_2 to yield a silica−carbon composite. The probable reactions involved in the formation of the silica−carbon composite from dimethyl polysiloxane in the presence of silica are given by

$$(-SiC_2H_6O-)_n + SiO_2 \xrightarrow{700\ ^\circ C} SiO_2 + SiO + 2C + 3H_2(g) \xrightarrow{air} 2SiO_2 + 2C$$

To understand the morphology of the silicaid grease, we carried out HR-SEM measurements. Since the grease was moving/decomposing under the field emission gun of HR-SEM, it was impossible to observe the silica filler or the components.

In conclusion, a nonaqueous, template-free, surfactant-free, and solvent-free approach was developed for the synthesis of a high surface area, conducting silica−carbon composite, using a commercial, low-cost, single precursor. Further annealing of the as-prepared SiO_2−carbon composite at 500 °C/air for 2 h led to the formation of white paramagnetic silica particles (confirmed by ESR) possessing a surface area of 111 m^2/g. The porous structure of the products was verified by HR-TEM and BET surface area measurements. The semi-graphitic carbon nature was also verified by HR-TEM and Raman measurements. The composition of the formed materials was verified by C, H, N, S analysis and EDX measurements, and the bulk conductivity of the SiO_2−carbon composite (5.72×10^{-6} $S \cdot cm^{-2}$) was determined by impedance measurements.

Acknowledgment. The authors thank Prof. Doron Aurbach and D. S. Jacob for their cooperation and help in the Raman measurements.

References and Notes

(1) Spange, S.; Muller, H.; Jager, C.; Bellmann, C. *Macromol. Symp.* **2002**, *177*, 111.

(2) (a) Diederich, F.; Rubin, Y. *Angew. Chem.* **1992**, *31*, 558. (b) Iijima, S.; *Nature* **1991**, *56*, 354.

(3) Ebbesen, T. W. *Acc. Chem. Res.* **1998**, *31*, 558.

(4) Scott, R. P. W. *Silica Gel and Bonded Phases*; John Wiley and Sons: New York, 1993.

(5) Iler, R. K. *The Chemistry of Silica*; John Wiley and Sons: New York, 1979.

(6) Han, C.-C.; Lee, J. T.; Yang, R. W.; Chang, H.; Han, H. C. H. *Chem. Commun.* **1998**, *11*, 2087.

(7) Miller, E. D.; Nesting, D. C.; Badding, J. V. *Chem. Mater.* **1997**, *9*, 18.

(8) Vohler, O.; Reiser, P. L.; Martina, R.; Overhoff, D. *Angew. Chem.* **1970**, *82*, 401.

(9) Kyotani, T.; Nagai, T.; Inoue, S.; Tomita, A. *Chem. Mater.* **1997**, *9*, 609.

(10) Han, S.; Hyeon, T. *Chem. Commun.* **1999**, 1955.

(11) Kyotani, T.; Sonoba, N.; Tomita, A. *Carbon* **1991**, *29*, 61.

(12) Muller, H.; Jager, C.; Rehak, P.; Meyer, N.; Hartmann, J.; Spange, S. *Adv. Mater.* **2000**, *12*, 1671.

(13) Kawashima, D.; Aihara, T.; Kobayashi, Y.; Kyotani, T.; Tomita, A. *Chem. Mater.* **2000**, *12*, 3397.

(14) Yitzhak, M.; Polarz, S.; Antonietti, M. *Adv. Funct. Mater.* **2002**, *12*, 197.

(15) Pang, J.; John, V. T.; Loy, D. A.; Yang, Z.; Lu, Y. *Adv. Mater.* **2005**, *17*, 704.

(16) Gilpin, R. K.; Gangoda, M. E.; Jaroniec, M. *Carbon* **1997**, *35*, 133.

(17) Chang, H.; Okuyama, K.; Szymanski, W. W. *Aerosol Sci. Technol.* **2003**, *37*, 735.

(18) Santra, S.; Bagwe, R. P.; Dutta, D.; Stanley, J. T.; Walter, G. A.; Tan, W.; Moudgil, B. M.; Mericle, R. A. *Adv. Mater.* **2005**, *17*, 2165.

(19) (a) Pol, V. G.; Pol, S. V.; Gedanken, A. *Chem. Mater.* **2005**, *17*, 1797. (b) Pol, S. V.; Pol, V. G.; Seisenbaeva, G.; Kessler, V. G.; Gedanken, A. *Chem. Mater.* **2004**, *16*, 1793. (c) Pol, V. G.; Pol, S. V.; Gedanken, A.; Goffer, Y. *J. Mater. Chem.* **2004**, *14*, 966. (d) Pol, V. G.; Calderon-Moreno, J.; Yoshimura, M.; Gedanken, A. *Carbon* **2004**, *42*, 111. (e) Pol, S. V.; Pol, V. G.; Gedanken, A. *Chem.—Eur. J.* **2004**, *10*, 4467. (f) Pol, S. V.; Pol, V. G.; Frydman, A.; Churilov, G. N.; Gedanken, A. *J. Phys. Chem. B* **2005**, *109*, 9495. (g) Pol, S. V.; Pol, V. G.; Kessler, V. G.; Seisenbaeva, G. A.; Sung, M.; Asai, S.; Gedanken, A. *J. Phys. Chem. B* **2004**, *108*, 6322. (h) Pol, S. V.; Pol, V. G.; Gedanken, A. *New J. Chem.* **2006**, *30*, 370. (i) Pol, S. V.; Pol, V. G.; Kessler, V. G.; Seisenbaeva, G. A.; Solovyov, L. A.; Gedanken, A. *Inorg. Chem.* **2005**, *44*, 9938.

(20) (a) Pol, V. G.; Pol, S. V.; Gedanken, A.; Sung, M.-G.; Shigeo, A. *Carbon* **2004**, *42*, 2738. (b) Pol, V. G.; Pol, S. V.; Gedanken, A. *J. Phys. Chem. B* **2005**, *109*, 6121.

(21) Stöber, W.; Fink, A.; Bohn, E. *J. Colloid Interface Sci.* **1968**, *26*, 62.

(22) Pol, V. G.; Srivastava, D. N.; Palchik, O.; Palchik, V.; Slifkin, M. A.; Weiss, A. M.; Gedanken, A. *Langmuir* **2002**, *18*, 3352.

(23) Kirk, C. T. *Phys. Rev. B* **1988**, *38*, 1255−1273.

(24) Dresselhaus, M. S.; Dresselhaus, G.; Pimenta, M. A.; Eklund, P. C. In *Analytical Application of Raman Spectroscopy*; Pelletier, M. J., Ed.; Blackwell Science: Oxford, 1999; Chapter 9.

(25) (a) Willard; Merrit; Dean. *Instrumental methods of analysis*, 5th ed.; 1974; p 236. (b) Mrozowski, S. *Carbon* **1979**, *17*, 227.

(26) Tatsumisago, M.; Honjo, H.; Sakai, Y.; Minami, T. *Solid State Ionics* **1994**, *74*, 105.

(27) Jacob, D. S.; Joseph, A.; Mallenahalli, S. P.; Shanmugam, S.; Makhluf, S.; Calderon-Moreno, J.; Koltypin, Y.; Gedanken A. *Angew. Chem., Int. Ed.* **2005**, *44*, 6560.